A Dysprosium Metallocene Single-Molecule Magnet Functioning at the Axial Limit

Fu-Sheng Guo,[a] Benjamin M. Day,[a] Yan-Cong Chen,[b] Ming-Liang Tong[b] Akseli Mansikkamäki[c] and Richard A. Layfield*[a]

Abstract: Abstraction of a chloride ligand from the dysprosium metallocene $[(Cp^{ttt})_2DyCl]$ ($\mathbf{1_{Dy}}$ Cp^{ttt} = 1,2,4-tri(*tert*-butyl)cyclopentadienide) by the triethylsilylium cation produces the first base-free rare-earth metallocenium cation $[(Cp^{ttt})_2Dy]^+$ ($\mathbf{2_{Dy}}$) as a salt of the non-coordinating $[B(C_6F_5)_4]^-$ anion. Magnetic measurements reveal that $[\mathbf{2_{Dy}}][B(C_6F_5)_4]$ is an SMM with a record anisotropy barrier up to 1277 cm^{-1} (1837 K) in zero field and a record magnetic blocking temperature of 60 K, including hysteresis with coercivity. The exceptional magnetic axiality of $\mathbf{2_{Dy}}$ is further highlighted by computational studies, which reveal this system to be the first lanthanide SMM in which all low-lying Kramers doublets correspond to a well-defined M_J value, with no significant mixing even in the higher doublets.

The drive to combine the macroscopic properties of bulk magnetic materials with the quantum effects observed in molecule-based materials has led to an explosion of interest in single-molecule magnets (SMMs).[1] In addition to the considerable fundamental interest in SMMs, several systems have been proposed for applications in nanoscale devices, such as molecular spin valves and spin transistors.[2] Molecule-based magnets offer the advantage of well-defined, tunable properties based on correlations that consider how the electronic structure of individual metal ions can be influenced by the coordination environment. For SMMs, the critical factors are now recognized as being the magnetic anisotropy of individual metal ions and the strength and the symmetry of the ligand field. Many of the most spectacular advances have therefore been achieved with lanthanide SMMs, especially complexes of the highly anisotropic Ln^{3+} cations of terbium, dysprosium, holmium and erbium.[3-6]

One of the most striking trends to have emerged recently is that improved properties can be achieved by targeting the synthesis of structurally simple monometallic SMMs rather than complex polynuclear compounds. This approach seemingly provides the most facile means of controlling the symmetry of the lanthanide coordination site, allowing progress towards SMM properties being observed at practical temperatures. A transformative breakthrough came with the report of slow magnetic relaxation in a D_{4d}-symmetric monometallic terbium phthalocyanine SMM,[7] with many derivatives of these systems showing enhanced properties such as larger effective energy barriers to reversal of the magnetization (the anisotropy barrier, U_{eff}) as a result of simple modifications to the ligand periphery.[8] A recent series of reports on D_{5h}-symmetric SMMs with the general formula $[Dy(OR)_2(L)_5]^+$ have produced huge U_{eff} values,[9] however even in these remarkable SMMs, the magnetic hysteresis properties typically feature zero-field quantum tunneling of the magnetization (QTM), which precludes potential applications in information storage.

Our contributions have focused on cyclopentadienyl-ligated dysprosium SMMs of the type $[(Cp)_2Dy(E)]_n$ (n = 2, 3) with various Cp ligands and a wide variety of heteroatom donor ligands, including systems with E = N, P, As, Sb, S and Se donors.[10] The key magneto-structural correlation arising from this work is that the $[Cp]^-$ ligands provide a dominant axial crystal field that enhances the magnetic anisotropy of Dy^{3+}, whereas the heteroatom donor ligands moderate the anisotropy, thus limiting U_{eff} and enabling zero-field QTM.[11] The logical conclusion from our studies is therefore that removing the equatorial ligands to give a discrete metallocenium cation of the type $[(Cp)_2Dy]^+$ should dramatically increase the anisotropy barrier *and* the blocking temperature, T_B.

Our strategy for targeting a base-free $[(Cp)_2Dy]^+$ cation as a salt of non-coordinating anions first sought to synthesize a compound of the type $[(Cp')_2MX]$, and then to abstract a halide ligand, X. In order to stabilize the putative cation, a bulky cyclopentadienide ligand was deemed necessary, therefore we opted for 1,2,4-tri(*tert*-butyl)cyclopentadienide (Cp^{ttt}). Halide abstraction from a hard lanthanide cation should require a highly electrophilic reagent, and the readily accessible triethylsilylium-containing salt $[(Et_3Si)_2(\mu\text{-}H)][B(C_6F_5)_4]$ was deemed to be an excellent candidate.[12] We reasoned that the driving force for halide abstraction would be greater with X = chloride, hence our initial target compound was $[(Cp^{ttt})_2DyCl]$ ($\mathbf{1_{Dy}}$) (Scheme 1). Compound $\mathbf{1_{Dy}}$ was synthesized by refluxing $[DyCl_3(THF)_{3.5}]$ with two equivalents of KCp^{ttt} in toluene for 72 hours. Subsequent work- up allowed $\mathbf{1_{Dy}}$ to be isolated as single crystals.

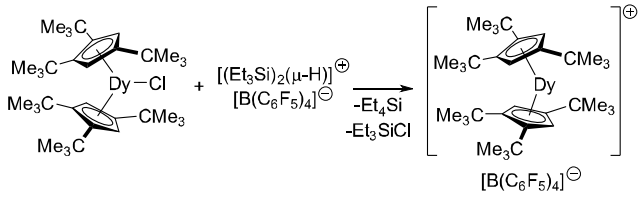

Scheme 1. Synthesis of $[\mathbf{2_{Dy}}][B(C_6F_5)_4]$ from $\mathbf{1_{Dy}}$.

[a] Dr F.-S. Guo, Dr B. M. Day, Prof. Dr R. A. Layfield
School of Chemistry
The University of Manchester
Oxford Road, Manchester, M13 9PL (U.K.)
E-mail: Richard.Layfield@manchester.ac.uk
[b] Y.-C. Chen, Prof. Dr M.-L. Tong
Key Laboratory of Bioinorganic and Synthetic Chemistry of the Ministry of Education, School of Chemistry
Sun-Yat Sen University
Guangzhou 510275 (P.R. China)
[c] A. Mansikkamäki
Department of Chemistry, Nanoscience Center
University of Jyväskylä
P.O. Box 35, Jyväskylä, FI-40014 (Finland)

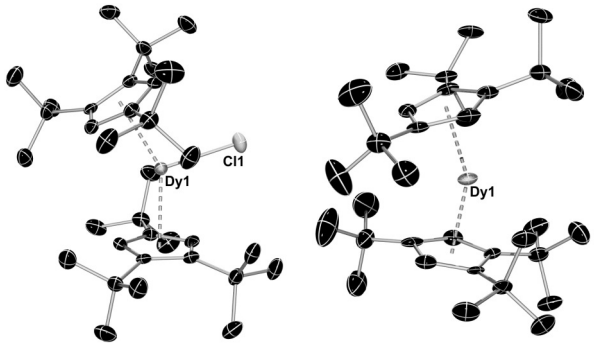

Figure 1. Molecular structure of $\mathbf{1_{Dy}}$ (left) and $\mathbf{2_{Dy}}$ (right). Thermal ellipsoids at 50% probability and hydrogen atoms omitted for clarity.

Crystallographic studies revealed that $\mathbf{1_{Dy}}$ adopts a bent metallocene structure with two symmetry-related Cp^{ttt} ligands (Figure 1, Table S1). The Dy–Cl distance is 2.5400(13) Å, the Dy–C distances are in the range 2.641(3)-2.781(3) Å, the Dy–Cp_c distance is 2.413(2) Å (Cp_c = ligand centroid), and the Cp_c-Dy-Cp_c angle is 147.59(7)°.

Chloride abstraction was achieved by adding a solution of $\mathbf{1_{Dy}}$ in hexane to a suspension of $[(Et_3Si)_2(\mu\text{-H})][B(C_6F_5)_4]$ at room temperature. The initially pale solution developed a yellow colour and rapidly deposited a yellow precipitate. Removal of the hexane *in vacuo* followed by addition of dichloromethane produced a bright yellow solution, from which $[(Cp^{ttt})_2Dy][B(C_6F_5)_4]$ ($[\mathbf{2_{Dy}}][B(C_6F_5)_4]$) was crystallized. The discrete cation $[(Cp^{ttt})_2Dy]^+$ ($\mathbf{2_{Dy}}$) also adopts a bent metallocene structure with the Dy–C bonds in the range 2.568(6)-2.711(7) Å, hence they are significantly shorter (by 0.06 Å) than those in $\mathbf{1_{Dy}}$ (Figure 1, Table S1). The Dy–Cp_c distances of 2.324(1) and 2.309(1) Å are also commensurately shorter owing to the greater electrostatic attraction of the Cp^{ttt} ligands to the low-coordinate dysprosium centre. The Cp_c-Dy-Cp_c angle in $\mathbf{2_{Dy}}$ is 152.845(2)°, hence overall the cation $\mathbf{2_{Dy}}$ is more compact and slightly closer to linearity than the metallocene unit in $\mathbf{1_{Dy}}$. Significantly, the shortest Dy···F distance in $[\mathbf{2_{Dy}}][B(C_6F_5)_4]$ is 5.8145(4) Å, which is far too long to represent even a weak bond, hence the counter anion is truly non-coordinating.

Metallocenium cations of formally tripositive metal ions are very rare for non-transition metals. Important examples include the aluminocenium cations, such as $[Cp_2Al]^+[MeB(C_6F_5)_3]^-$, which is an initiator for the cationic polymerization of isobutene.[13] The cation $\mathbf{2_{Dy}}$ is the first rare-earth and the first f-block metallocenium cation. The only other base-free rare-earth bis(cyclopentadienyl) complexes are those of the limited selection of stable divalent lanthanides, such as the archetypal compound decamethylsamarocene.[14] Although related to $\mathbf{2_{Dy}}$, the rare-earth contact ion-pairs $[(Cp^*)_2M(\mu\text{-Ph})_2BPh_2]$ show well-defined cation-π bonding interactions between the tetraphenylborate anion and the metal.[15]

The temperature dependence of $\chi_M T$, where χ_M is the molar magnetic susceptibility, was measured for $\mathbf{1_{Dy}}$ and $[\mathbf{2_{Dy}}][B(C_6F_5)_4]$ in an applied field of 1000 Oe. The results are typical of monometallic Dy^{3+} complexes, and show similar steady decreases down to about 50 K (Figures S2, S3). At lower temperatures, a marked difference in the decrease in $\chi_M T$ was observed: for $\mathbf{1_{Dy}}$, the decrease continues gradually, whereas for $[\mathbf{2_{Dy}}][B(C_6F_5)_4]$ a precipitous drop occurs, which is indicative of strong magnetic blocking. Investigating the AC magnetic susceptibilty of $\mathbf{1_{Dy}}$ revealed that the QTM in this system is very severe (Figure S4). The frequency (ν) dependence of the out-of-phase magnetic susceptibility (χ'') for $\mathbf{1_{Dy}}$ showed no maxima at any temperature accessible by our SQUID magnetometer, hence it was not possible to extract an anisotropy barrier for this compound. The field-dependence of the magnetization for $\mathbf{1_{Dy}}$ showed a typical S-shaped curve with only very small openings at fields of $H \approx 0.1$-1.0 T (Figure S5).

In stark contrast, the AC susceptibility studies on $[\mathbf{2_{Dy}}][B(C_6F_5)_4]$ using an oscillating field of 5 Oe show peaks in $\chi''(\nu)$ at temperatures of 72-110 K in zero applied field, with the position of the peaks showing a strong dependence on temperature and on the AC frequency (Figures 2, S6). From this data, Cole-Cole plots of χ'' versus χ' were obtained and fitted using a generalized Debye model (Figure S7), which produced α-parameters in the range 0-0.036, indicating an extremely narrow distribution of relaxation times. Further analysis of this data by plotting the relaxation time, τ, as a function of reciprocal temperature produced a linear relationship, revealing that the magnetic relaxation in $[\mathbf{2_{Dy}}][B(C_6F_5)_4]$ proceeds solely via a thermal mechanism (Figure 2). Fitting the data to the Arrhenius law $\tau^{-1} = \tau_0^{-1} e^{-U_{\text{eff}}/k_B T}$ yielded a new record barrier of U_{eff} = 1277(14) cm^{-1} ($\tau_0 = 8.12 \times 10^{-12}$ s), slightly surpassing the previous record set by $[Dy(O^tBu)_2(py)_5]^+$.[9a]

To probe the magnetic relaxation behaviour at lower temperatures, DC magnetic measurements were employed in order to extract relaxation times from plots of the remnant magnetization as a function of time (Figure S8). The result of this analysis is that the linear dependence of τ on T persists down to 53 K, which, strikingly, corresponds to a relaxation time of τ = 100 s, and can therefore be used to define the magnetic blocking temperature, T_B, for $\mathbf{2_{Dy}}$.[3] The most notable recent example of an SMM for which comparable data were reported is a the radical-bridged species $[Tb_2(N_2)\{N(SiMe_3)_2\}_4(thf)_2]^-$,[3] which has a 100 s blocking temperature of only 13.9 K, hence the blocking temperature for $[\mathbf{2_{Dy}}][B(C_6F_5)_4]$ is by far the largest ever reported, and provides a major advance towards the development of SMMs that function above the symbolic temperature 77 K, at which nitrogen liquefies. In the extended low temperature range, the relaxation develops a slight curvature, suggesting that Raman relaxation is more dominant. The equation $\tau^{-1} = \tau_0^{-1} e^{-U_{\text{eff}}/k_B T} + CT^n$, in which C and n are the Raman parameters, was used to fit the full range data. This analysis produced U_{eff} = 1256(14) cm^{-1}, $\tau_0 = 1.09 \times 10^{-11}$ s, $C = 1.81 \times 10^{-9}$ s^{-1} K^{-n} and n = 3.92(0.38).

Another definition of blocking temperature is the temperature at which the field-cooled (FC) and zero-field-cooled (ZFC) magnetic susceptibility diverge.[9a] For $[\mathbf{2_{Dy}}][B(C_6F_5)_4]$, this divergence occurs at 60 K, which further illustrates the magnetization blocking and is broadly consistent with the temperature when the relaxation time is 100 s (Figure S9). The true magnet-like credentials of $[\mathbf{2_{Dy}}][B(C_6F_5)_4]$ were established by measuring the field-dependence of the magnetization using an average field sweep rate of 3.9 mT s^{-1} (39 Oe s^{-1}).

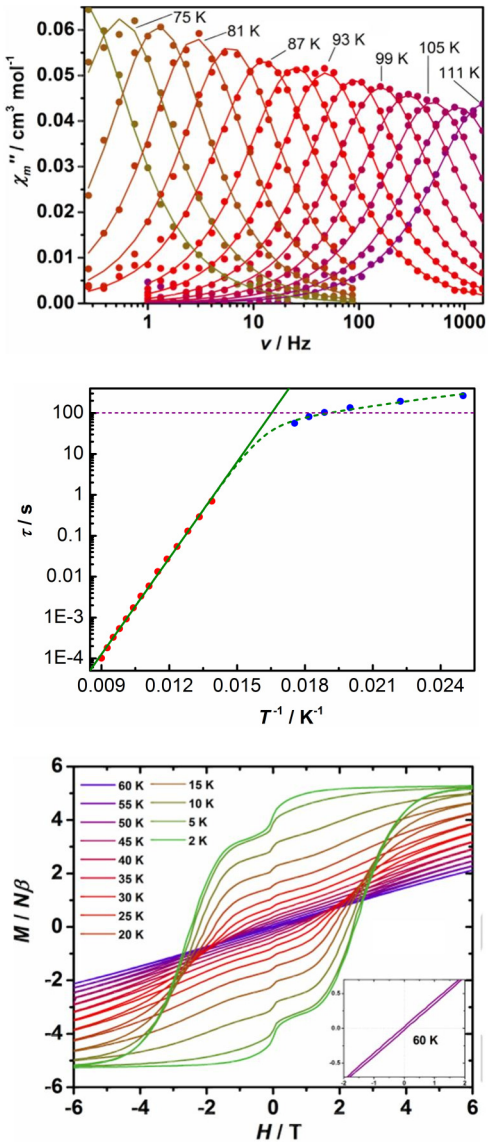

Figure 2. Upper: $\chi''(\nu)$ in zero applied field for $\mathbf{2_{Dy}}$ and various temperatures in the range 60-123 K using 3 K intervals. Middle: Temperature dependence of the relaxation time for $\mathbf{2_{Dy}}$, where solid lines are fits using the parameters in the text: red points are from the AC susceptibility and blue points from DC magnetic relaxation measurements. Lower: $M(H)$ hysteresis for $\mathbf{2_{Dy}}$ using an average sweep rate of 3.9 mT s^{-1}.

Under these conditions, the results are remarkable, with the $M(H)$ loops remaining open up to 60 K, which is substantially higher than any previously observed hysteresis in an SMM (Figures 2, S10). Even more remarkable is the coercive field of H_c = 0.06 T at 60 K. At temperatures of 55-2 K, the hysteresis loops are wider still, with the coercive fields in the range 0.19-2.46 T. Although comparisons of hysteresis measured for SMMs are rendered complicated by the use of different sweep rates, it is clear that the hysteresis properties of $[\mathbf{2_{Dy}}][B(C_6F_5)_4]$ surpass those of the radical-bridged di-terbium species[3] and of the D_{5h}-symmetric dysprosium complexes,[9] and therefore that our system is the new benchmark for the field.

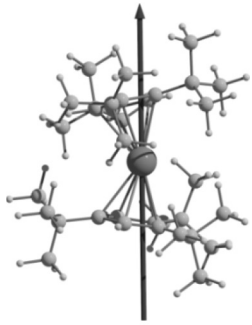

Figure 3. Direction of the principal axis of the g-tensor in the ground KD of $\mathbf{2_{Dy}}$.

Detailed insight into the magnetic properties of $\mathbf{1_{Dy}}$ and $\mathbf{2_{Dy}}$ was obtained through *ab initio* calculations, which used the experimentally determined atomic coordinates for all heavy atoms, with the positions of hydrogen atoms being optimized at the DFT level. The energies of the eight lowest Kramers doublets (KDs) of $\mathbf{1_{Dy}}$ and $\mathbf{2_{Dy}}$ of the $^6H_{15/2}$ multiplet of Dy^{3+}, along with the principal components of the respective g-tensors and the angles between the ground and excited doublets are listed in Table S2. The principal axes of the ground doublets in $\mathbf{1_{Dy}}$ and $\mathbf{2_{Dy}}$ are oriented towards the centres of the $[Cp^{ttt}]^-$ ligands (Figures 3, S11), in broad agreement with a theoretical study on the hypothetical species $[(Cp^*)_2Dy]^+$.[16] Focusing on $\mathbf{2_{Dy}}$, all except the eighth KD have almost axial g-tensors. Up to the fourth KD, the tensors are essentially perfectly axial, and the axiality remains high in the fifth KD. Above this, the transverse components of the g-tensor become significant, and in the eighth KD the g_x component dominates. All excited KDs are roughly parallel with the ground doublet, with the largest deviation of 5.6° being that between the ground and the fifth KDs. In contrast, the ground doublet in $\mathbf{1_{Dy}}$ has a fairly axial g-tensor with small but non-negligible transverse components, suggesting that this tensor is not axial enough to sufficiently suppress quantum tunneling of magnetization (QTM) within the ground doublet, as observed experimentally.[17]

The splitting of the $^6H_{15/2}$ multiplets in $\mathbf{1_{Dy}}$ and $\mathbf{2_{Dy}}$ was further studied by calculating the decomposition of the SO-RASSI wave functions of the eight lowest KDs into projections onto the $|JM_J>$ states, where J = 15/2 (Table S3).[18] Significantly, in $\mathbf{2_{Dy}}$ each of the sixteen lowest states has a large projection onto one given $|JM_J>$ state. The smallest projection is 0.964 in the sixth KD with M_J = ±5/2. All the crystal field states of the $^6H_{15/2}$ multiplet in $\mathbf{2_{Dy}}$ can therefore be assigned to one M_J value, and no significant mixing between the states occurs. To the best of our knowledge, this is the closest to a perfectly axial crystal field observed in any molecular lanthanide complex. In contrast, the equatorially coordinated chloride in 1_{Dy} leads to strong mixing between states with different M_J projections. Although projections onto the M_J = ±15/2 states in the ground doublet are still fairly large (0.909), in the first excited doublet the projection onto the M_J = ±13/2 states are only 0.586, and beyond this the states are strongly mixed.

Based on the calculations, mechanisms for the relaxation of magnetization in $\mathbf{1_{Dy}}$ and $\mathbf{2_{Dy}}$ can be proposed (Figures 4, S12).[19] In $\mathbf{1_{Dy}}$, the matrix elements connecting the M_J = ±15/2

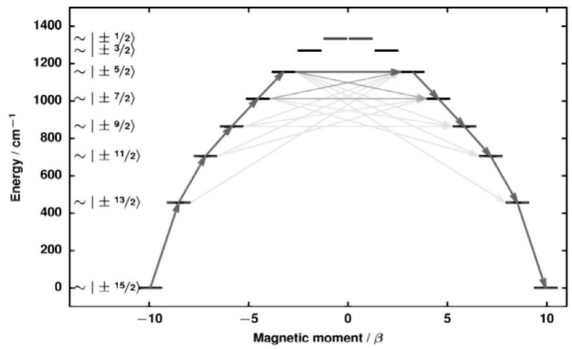

Figure 4. Relaxation of the magnetization in $\mathbf{2_{Dy}}$. Dark grey arrows show the most probable relaxation route and light grey arrows indicate less significant but non-negligible matrix elements between states.

states are substantial, hence ground-state QTM is highly efficient and represent the dominant relaxation process. In $\mathbf{2_{Dy}}$, the QTM is effectively blocked in the ground doublet and the first two excited doublets. Starting from the ground doublet, the transition matrix element grows roughly an order of magnitude within each following doublet, in agreement with the increasing transverse components of the respective *g*-tensors. The QTM starts to become non-negligible in the fourth KD, and in the sixth KD it is dominant. The energy of the sixth doublet (1156 cm^{-1}) agrees well with the experimentally observed effective barrier height (1277 cm^{-1}). The almost perfectly linear temperature dependence of τ (Figure 2) suggests that Raman processes are not significant above the blocking temperature, and the effective barrier height should correspond to the energy of the highest doublet involved in the relaxation mechanism. The energy of the seventh doublet (1270 cm^{-1}) is closer to the experimental value than that of the sixth doublet, however, the strong QTM in the sixth doublet makes it extremely unlikely that the relaxation would proceed via any higher doublet. The small deviation between the energy of the sixth doublet and U_{eff} most likely results from neglecting electron correlation outside the 4f orbital space in the CASSCF calculations.

In summary, the complex cation $[(Cp^{ttt})_2Dy]^+$ ($\mathbf{2_{Dy}}$) gives rise to unprecedented single-molecule magnet properties, including a record anisotropy barrier and, more notably, magnetic blocking temperatures and coercivity that far exceed, those described for all previous SMMs. The properties of $\mathbf{2_{Dy}}$ arise from the exceptional magnetic axiality of Dy^{3+} in the *bis*(cyclopentadienyl) ligand environment. Theoretical studies of $\mathbf{1_{Dy}}$ and $\mathbf{2_{Dy}}$ have provided clear insight into the origins of the facile QTM in the former and the effective suppression of QTM in the latter, leading to dominant relaxation via the sixth Kramers doublet. Having established a new benchmark in molecular magnetism that pushes the blocking temperature much closer to the symbolic temperature of 77 K, the next challenge is to develop new SMMs with properties that exceed those of $\mathbf{2_{Dy}}$.

Acknowledgements

The authors thank: the UK EPSRC (Fellowship to RAL, postdoctoral funding to BDM); the European Commission (MSCA Fellowship to FSG); the NSFC (YCC and MLT, projects 21620102002, 91422302); the Academy of Finland (funding for AM, project 282499); and Prof. H. M. Tuononen (University of Jyväskylä) for providing computational resources.

Keywords: dysprosium • single-molecule magnet • anisotropy • organometallics • cyclopentadienyl ligands

[1] a) J. M. Frost, K. L. M. Harriman, M. Murugesu, *Chem. Sci.* **2016**, *7*, 2470. b) P. Zhang, L. Zhang, J. Tang, *Dalton Trans.* **2015**, *44*, 3923. c) D. N. Woodruff, R. E. P. Winpenny, R. A. Layfield, *Chem. Rev.* **2013**, *113*, 5110.

[2] a) R. Vincent, S. Klyatskaya, M. Ruben, W. Wernsdorfer, F. Balestro, *Nature*, **2012**, *488*, 357. b) M. Shiddiq, D. Komijani, Y. Duan, A. Gaita-Ariño, E. Coronado, S. Hill, *Nature*, **2016**, *531*, 348.

[3] J. D. Rinehart, M. Fang, W. J. Evans, J. R. Long, *J. Am. Chem. Soc.* **2011**, *133*, 14236.

[4] a) S. K. Langley, D. P. Wielechowski, V. Vieru, N. F. Chilton, B. Moubaraki, B. F. Abrahams, L. F. Chibotaru, K. S. Murray, *Angew. Chem. Int. Ed.* **2013**, *52*, 12014. b) K. L. M. Harrima, J. L. Brosmer, L. Ungur, P. L. Diaconescu, M. Murugesu, *J. Am. Chem. Soc.* **2017**, *139*, 1420.

[5] Y.-C. Chen, J.-L. Liu, W. Wernsdorfer, D. Liu, L. F. Chibotaru, X.-M. Chen, M.-L. Tong, *Angew. Chem. Int. Ed.* **2017**, *56*, 4996.

[6] a) P. Zhang, L. Zhang, C. Wang, S. Xue, S.-Y. Lin, J. Tang, *J. Am. Chem. Soc.* **2014**, *136*, 4484. b) L. Ungur, J. J. Le Roy, I. Korobkov, M. Murugesu, L. F. Chibotaru, *Angew. Chem. Int. Ed.* **2014**, *53*, 4413.

[7] a) N. Ishikawa, M. Sugita, T. Ishikawa, S. Koshihara Y. Kaizu, *J. Am. Chem. Soc.* **2003**, *125*, 8694. b) Z. Liang, M. Damjanović, M. Kamila, G. Cosquer, B. K. Breedlove, M. Enders, M. Yamashita, *Inorg. Chem.* **2017**, *56*, 6512.

[8] C. R. Ganivet, B. Ballasteros, G. de la Torre, J. M. Clemente-Juan, E. Coronado, T. Torres, *Chem. Eur. J.* **2013**, *19*, 1457.

[9] a) Y.-S. Ding, N. F. Chilton, R. E. P. Winpenny, Y.-Z. Zheng, *Angew. Chem. Int. Ed.* **2016**, *55*, 16071. b) Y.-C. Chen, J.-L. Liu, L. Ungur, J. Liu, Q.-W. Li, L.-F. Wang, Z.-P. Ni, L. F. Chibotaru, X.-M. Chen, M.-L. Tong, *J. Am. Chem. Soc.* **2016**, *138*, 2829. c) S. K. Gupta, T. Rajeshkumar, G. Rajaraman, R. Murugavel, *Chem. Sci.* **2016**, *7*, 5181.

[10] a) R. A. Layfield, J. J. W. McDouall, S. A. Sulway, D. Collison, F. Tuna, R. E. P. Winpenny, *Chem. Eur. J.* **2010**, *16*, 4442. b) T. Pugh, F. Tuna, L. Ungur, D. Collison, E. J. L. McInnes, L. F. Chibotaru, R. A. Layfield, *Nat. Commun.* **2015**, *6*, 7492. c) T. Pugh, V. Vieru, L. F. Chibotaru, R. A. Layfield, *Chem. Sci.* **2016**, *7*, 2128. d) T. Pugh, N. F. Chilton, R. A. Layfield, *Chem. Sci.* **2017**, *8*, 2073.

[11] T. Pugh, N. F. Chilton, R. A. Layfield, *Angew. Chem. Int. Ed.* **2016**, *55*, 11082.

[12] S. J. Connelly, W. Kaminsky, D. M. Heinekey, *Organometallics* **2013**, *32*, 7478.

[13] M. Bochmann, D. Dawson, *Angew. Chem. Int. Ed.* **1996**, *35*, 2226.

[14] a) C. Ruspic, J. R. Moss, M. Schurmann, S. Harder, *Angew. Chem. Int. Ed.* **2008**, *47*, 2121. b) W. J. Evans, L. A. Hughes T. P. Hanusa, *J. Am. Chem. Soc.* **1984**, *106*, 4270.

[15] S. E. Lorenz, B. M. Schmiege, D. S. Lee, J. W. Ziller W. J. Evans, *Inorg. Chem.* **2010**, *49*, 6655.

[16] Y.-S. Meng, Y.-Q. Zhang, Z.-M. Wang, B.-W. Wang S. Gao, *Chem. Eur. J.* **2016**, *22*, 12724

[17] L. Ungur, L. F. Chibotaru. *Phys. Chem. Chem. Phys.* **2011**, *13*, 20086.

[18] L. Ungur, L. F. Chibotaru. *Chem. Eur. J.* **2017**, *23*, 3708.

[19] L. Ungur, M. Thewissen, J.-P. Costes, W. Wernsdorfer, L. F. Chibotaru. *Inorg. Chem.*, **2013**, *52*, 6328.